

## Counterions at Highly Charged Interfaces: From One Plate to Like-Charge Attraction

Ladislav Šamaj\* and Emmanuel Trizac

*Laboratoire de Physique Théorique et Modèles Statistiques, UMR CNRS 8626, Université Paris-Sud, 91405 Orsay, France*

(Received 28 July 2010; published 18 February 2011)

We present an analytical approach for similarly and highly charged planar interfaces in the presence of counterions. The procedure is physically transparent and based on an exact low temperature expansion around the ground state formed by the two-dimensional Wigner crystal of counterions. The one plate problem is worked out, together with the two plates situation. Unlike previous approaches, the expansion is free of divergences, and is shown to be in excellent agreement with available data of Monte Carlo simulations under strong Coulombic couplings. In the two plates case, the present results shed light on the like-charge attraction regime.

DOI: 10.1103/PhysRevLett.106.078301

PACS numbers: 82.70.-y, 61.20.Qg, 82.45.-h

The behavior of charged particles in the vicinity of charged interfaces is a central yet elusive problem in the equilibrium statistical mechanics of Coulomb fluids, including colloidal science. A landmark in the field was the realization in the 1980s that similarly charged surfaces may attract each other under strong enough Coulombic couplings, which can be realized in practice increasing the valency of the counterions involved [1]. Notorious illustrations of this like-charge attraction are the formation of DNA condensates [2] or aggregates of colloidal particles [3].

The weak-coupling limit is described by the Poisson-Boltzmann mean-field approach [4] and by its systematic improvements via the loop expansion [5–7]. A remarkable achievement of the past decade has been accomplished in the opposite strong-coupling (SC) limit, pioneered by Rouzina and Bloomfield [8], substantiated by Shklovskii, Levin, and collaborators [9], and formalized by Netz and collaborators [10–12]. An essential ingredient is that the layer of counterions close to a charged wall becomes two dimensional, and in the field-theoretical method put forward in [10,11], the leading behavior stems from a single-particle theory, which produces more compact profiles than within mean-field theory [13]. Next correction orders correspond to a virial or fugacity expansion in inverse powers of the coupling constant  $\Xi$ , to be defined below. The method requires a renormalization of infrared divergences via the electroneutrality condition. A comparison with Monte Carlo (MC) simulations [10] indicates the adequacy of the virial SC approach to capture the leading large  $\Xi$  order, but its failure for the first correction.

The establishment of an (approximative) interpolation between the Poisson-Boltzmann and SC regimes, based on the idea of a “correlation hole,” was the subject of a series of works [14–17]. A relevant observation in [17], corroborated by a comparison with the MC simulations, was that the first correction in the SC expansion is proportional to  $1/\sqrt{\Xi}$ , and not to  $1/\Xi$  as suggested in [10,11].

The aim of this Letter is to revisit highly charged interfaces and establish an exact expansion which, in light of

the previous discussion, has yet to be formulated. The leading term of counterion density profiles coincides with the single-particle picture of the original virial SC works. Our expansion is free of infrared divergences and entails a correction in  $1/\sqrt{\Xi}$  to the leading behavior, thus formally corresponding to the lowest order expansion in terms of the temperature. Our analytical results are shown to be in excellent agreement with available MC data without adjustable parameters. Our procedure is versatile. It yields new exact results in the like-charge attraction regime and is, as such, relevant for practical applications such as the stability of cement pastes [18].

Here, we study a classical system of (equally charged) counterions in the vicinity of one or two planar walls bearing a uniform surface-charge density,  $\sigma e$  ( $e$  is the elementary charge and  $\sigma > 0$ ), the system as a whole being electroneutral. The system, at thermal equilibrium at the inverse temperature  $\beta = 1/(k_B T)$ , is immersed in a solution of dielectric constant  $\epsilon$  containing  $q$ -valent counterions, each thus having charge  $-qe$ . For simplicity, no image forces are present. Let us describe briefly the original approach of [10,11] for the case of a single wall localized in the  $z = 0$  plane. The counterions are confined to the half-space  $z \geq 0$ . The relevant length scales in Gaussian units are the Bjerrum length  $\ell_B = \beta e^2/\epsilon$ , i.e., the distance at which two unit charges interact with thermal energy  $k_B T$ , and the Gouy-Chapman length  $\mu = 1/(2\pi q \ell_B \sigma)$ , i.e., the distance from the charged wall at which an isolated counterion has potential energy equal to thermal energy. All lengths  $r$  will be expressed in units of  $\mu$ ,  $\tilde{r} = r/\mu$ . The counterion density profile  $\rho(z)$ , which only depends on the distance from the wall  $z$ , will be considered in the rescaled form  $\tilde{\rho}(\tilde{z}) = \rho(\mu\tilde{z})/(2\pi\ell_B\sigma^2)$ , so that the electroneutrality condition  $q \int_0^\infty dz \rho(z) = \sigma$  simply reads  $\int_0^\infty d\tilde{z} \tilde{\rho}(\tilde{z}) = 1$ . The coupling parameter quantifying the strength of electrostatic correlations is  $\Xi = 2\pi q^3 \ell_B^2 \sigma$ ; it will play the role of our expansion parameter. According to the virial SC approach [10,11], the counterion density profile can be formally expanded as

$$\tilde{\rho}(\tilde{z}) = \tilde{\rho}_0(\tilde{z}) + \frac{1}{\theta} \tilde{\rho}_1(\tilde{z}) + O(\Xi^{-2}), \quad (1)$$

where

$$\tilde{\rho}_0(\tilde{z}) = e^{-\tilde{z}}, \quad \tilde{\rho}_1(\tilde{z}) = e^{-\tilde{z}}(\tilde{z}^2/2 - \tilde{z}), \quad (2)$$

with  $\theta = \Xi$ . The leading term  $\tilde{\rho}_0(\tilde{z})$  comes from the single-particle picture of counterions in the linear surface-charge potential. The MC simulations [10] indicate that the first correction  $\tilde{\rho}_1(\tilde{z})$  has the expected functional form for  $\Xi > 10$ ; however, the value of the prefactor is incorrect. The simulations indeed reveal that  $\theta \neq \Xi$ , see the inset of Fig. 1, where the prefactor  $\theta$  extracted from MC simulations following Eq. (1) is much smaller than  $\Xi$ .

Our approach is based on the fact that in the asymptotic limit  $\Xi \rightarrow \infty$  the counterions collapse on the charged surface, creating a 2D hexagonal (equilateral triangular) Wigner crystal [9] where every ion has 6 nearest neighbors forming a hexagon. Let us denote by  $\mathbf{R}_i = (X_i, Y_i)$  the position vectors of the vertices on this hexagonal lattice. Since there are just two triangles per particle, the lattice spacing  $a$  of the globally electroneutral structure is given by  $q/\sigma = \sqrt{3}a^2/2$ . Note that the large  $\Xi$  limit coincides with the regime in which the distance  $a$  between the nearest-neighbor counterions is much larger than the distance  $\mu$  between the counterions and the charged surface [8],  $\tilde{a} \equiv a/\mu \propto \sqrt{\Xi} \gg 1$ . When  $\Xi \rightarrow \infty$ , each vertex  $\mathbf{R}_i$  is occupied by a counterion  $i$  ( $i = 1, \dots, N$ ;  $N \rightarrow \infty$ ). The ground-state energy of the counterion system together with the homogeneous background charge is  $E_0$ . For  $\Xi$  large but not infinite, the fluctuations of ions around their lattice positions begin to play a role [19].

Let us first shift one of the particles, say  $i = 1$ , from its lattice position  $\mathbf{R}_1$  by a small vector  $\delta\mathbf{R}_1 = (x, y, z)$  ( $\delta R_1 \equiv |\delta\mathbf{R}_1| \ll a$ ) and look for the corresponding change in the total energy  $\delta E = E - E_0 \geq 0$ . The first contribution to  $\delta E$  comes from the interaction of the

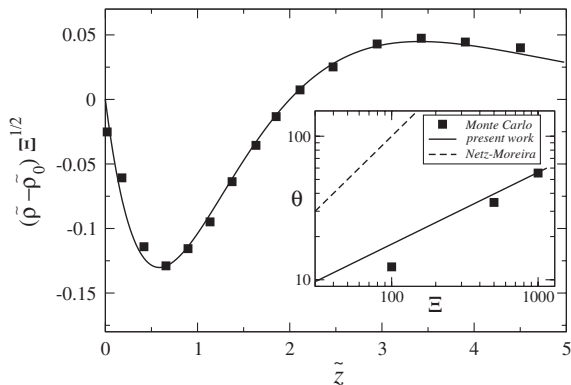


FIG. 1. Comparison between the analytical first correction to the profile  $\tilde{\rho}_0$  (solid curve) and the Monte Carlo results of Ref. [10] at  $\Xi = 10^3$ , for a single charged wall. The inset compares our prediction for the rescaling factor  $\theta$  [solid curve given by Eq. (9)] to its Monte Carlo value reported in [10] and to the original virial SC prediction  $\theta = \Xi$  (dashed line).

shifted counterion with the potential induced by the homogeneous surface-charge density:  $\delta E^{(1)} = 2\pi q e^2 \sigma z / \epsilon$ . The second contribution to  $\delta E$  comes from the interaction of the particle with all other particles on the 2D hexagonal lattice. This contribution can be expanded as an infinite series in  $x$ ,  $y$ , and  $z$ ; for our purposes, it is sufficient to consider this expansion up to harmonic terms, which, in the  $z$  direction, read

$$\epsilon \delta E_z^{(2)} = \sum_{i \neq 1} \left[ \frac{(qe)^2}{\sqrt{R_i^2 + z^2}} - \frac{(qe)^2}{R_i} \right] \sim -\frac{(qe)^2}{2a^3} S z^2. \quad (3)$$

Here, the dimensionless quantity  $S = \sum_{i \neq 1} (R_i/a)^{-3}$  can be expressed from the general theory of lattice sums [20]

$$S = \sum_{\substack{m,n=-\infty \\ (m,n) \neq (0,0)}}^{\infty} \frac{1}{(m^2 + mn + n^2)^{3/2}} \\ = \frac{2}{\sqrt{3}} \zeta\left(\frac{3}{2}\right) \left[ \zeta\left(\frac{3}{2}, \frac{1}{3}\right) - \zeta\left(\frac{3}{2}, \frac{2}{3}\right) \right], \quad (4)$$

where  $\zeta(z, q) = \sum_{n=0}^{\infty} 1/(q+n)^z$  is the generalized Riemann zeta function and  $\zeta(z) \equiv \zeta(z, 1)$ . Explicitly,  $S = 11.034 \dots$ . A shift of the particle simultaneously along all directions does not induce “mixed” harmonic terms of type  $xz$  or  $yz$ . The harmonic term in the  $(x, y)$  plane can be computed, and in dimensionless form, we have

$$-\beta \delta E \sim -\tilde{z} + \frac{3^{3/4}}{(4\pi)^{3/2}} \frac{S}{\sqrt{\Xi}} \left[ \frac{\tilde{z}^2}{2} - \frac{1}{4}(\tilde{x}^2 + \tilde{y}^2) \right]. \quad (5)$$

This formula reveals a relationship between the order of the expansion of  $-\beta \delta E$  in the dimensionless lengths  $\tilde{x}$ ,  $\tilde{y}$ ,  $\tilde{z}$  and the expansion in  $1/\sqrt{\Xi}$ . The linear term  $-\tilde{z}$ , which is the only one which does not vanish in the limit  $\Xi \rightarrow \infty$ , is the leading term. It corresponds to the single-particle picture, in close analogy with the previous virial SC approach. The harmonic terms turn out to be of order  $\beta(qe)^2 \mu^2/a^3 \propto 1/\sqrt{\Xi}$ , and likewise, terms of the  $p$ th order in the variables  $\tilde{x}$ ,  $\tilde{y}$ ,  $\tilde{z}$  are of order  $\beta(qe)^2 \mu^p/a^{p+1} \propto 1/\Xi^{(p-1)/2}$ . This scheme constitutes a systematic basis for our large  $\Xi$  expansion.

The generalization of the above formalism to all particles is straightforward. We shift every particle  $i = 1, 2, \dots, N$  from its lattice position  $\mathbf{R}_i$  by a small vector  $\delta\mathbf{R}_i = (x_i, y_i, z_i)$ . In what follows, however, we shall be interested in the counterion density profile which only depends on the  $\tilde{z}$  coordinate. Thus, when expanding in statistical averages the Gibbs weight  $\exp(-\beta \delta E)$  in powers of  $1/\sqrt{\Xi}$ , we can restrict ourselves to the  $z$ -harmonic part. The corresponding change in the total energy  $\delta E$  is given by a counterpart of (5),

$$-\beta \delta E \sim -\sum_i \tilde{z}_i + \frac{3^{3/4}}{16\pi^{3/2}} \frac{1}{\sqrt{\Xi}} \sum_{i < j} \frac{(\tilde{z}_i - \tilde{z}_j)^2}{(|\mathbf{R}_i - \mathbf{R}_j|/a)^3}. \quad (6)$$

The next simplification comes from the fact that particles are identical, exposed to the same potential induced by the

surface charge, so that a summation over particle coordinates can be represented by just one auxiliary coordinate. For the density particle profile, defined by  $\rho(\mathbf{r}) = \langle \sum_{i=1}^N \delta(\mathbf{r} - \mathbf{r}_i) \rangle = N \langle \delta(\mathbf{r} - \mathbf{r}_1) \rangle$ , we get explicitly

$$\tilde{\rho}(\tilde{z}) = C e^{-\tilde{z}} \int_0^\infty d\tilde{z}' e^{-\tilde{z}'} \left[ 1 + \frac{3^{3/4} S}{16\pi^{3/2}} \frac{(\tilde{z} - \tilde{z}')^2}{\sqrt{\Xi}} \right] + O\left(\frac{1}{\Xi}\right), \quad (7)$$

where  $C$  is determined by the normalization condition  $\int \tilde{\rho} = 1$ . Simple algebra gives

$$\tilde{\rho}(\tilde{z}) = e^{-\tilde{z}} + \frac{3^{3/4}}{(4\pi)^{3/2}} \frac{S}{\sqrt{\Xi}} e^{-\tilde{z}} \left( \frac{\tilde{z}^2}{2} - \tilde{z} \right) + O(\Xi^{-1}). \quad (8)$$

Comparing this result with Eqs. (1) and (2) obtained in the virial SC approach [10,11], we see that the leading terms coincide, while the first corrections have the same functional dependence in space but different prefactors. The result (8) can be reexpressed in terms of the  $\theta$  factor, introduced in the relation (1), as follows:

$$\theta = \frac{(4\pi)^{3/2}}{3^{3/4}} \frac{1}{S} \sqrt{\Xi} = 1.771 \dots \sqrt{\Xi}. \quad (9)$$

This formula, in excellent agreement with MC data, differs substantially from the previous virial SC estimate  $\theta = \Xi$ ; see Fig. 1.

The method can be readily applied to the case of two parallel walls, each having the same charge density  $\sigma e$ , located at distance  $d$  from one another. The electric field between the walls is equal to 0 now. At  $T = 0$ , the classical system is defined by the dimensionless separation  $\eta = d\sqrt{\sigma/q} = \tilde{d}/\sqrt{2\pi\Xi}$ . A complication comes from the fact that counterions form, on the opposite surfaces, a bilayer Wigner crystal, the structure of which depends on  $\eta$  [21–23]. We implement our expansion as the limit of large  $\Xi$  at fixed  $\tilde{d}$ , which means that  $\eta \propto \tilde{d}/\sqrt{\Xi} \rightarrow 0$ . In this limit, the relevant ground-state structure is that of the single hexagonal lattice [so-called structure I, see Fig. 2 (left), where open and filled symbols are for ions on opposite surfaces]. Because of global neutrality, the lattice spacing  $b$  of the single (bilayer) hexagonal structure is given by  $q/(2\sigma) = \sqrt{3}b^2/2$ .

The two walls are located at positions  $z = 0$  and  $z = d$ . The position vector  $\mathbf{R}_i$  of the particle localized on the shared hexagonal Wigner lattice will be denoted as  $\mathbf{R}_i^{(0)}$  if it belongs to the wall at  $z = 0$  (say, filled symbols of the left-hand panel of Fig. 2) and as  $\mathbf{R}_i^{(d)}$  if it belongs to the wall at  $z = d$  (open symbols in Fig. 2). Let us shift the particle  $i = 1$  localized on the  $z = 0$  wall by a small vector  $\delta\mathbf{R}_1^{(0)} = (x, y, z)$  and look for the energy change  $\delta E$  from the ground state. Since the potential induced by the surface charge on the walls is constant between the walls, the corresponding  $\delta E^{(1)} = 0$ . The harmonic term in the  $z$  direction reads

$$\epsilon \delta E_z^{(2)} = \frac{(qe)^2}{2b^3} \left[ - \sum_{i \neq 1} \frac{z^2}{(R_i^{(0)}/b)^3} + \sum_i \frac{d^2 - (d-z)^2}{(R_i^{(d)}/b)^3} \right]. \quad (10)$$

Using the exact values of the partial hexagonal sums [20]  $\sum_{i \neq 1} [b/R_i^{(0)}]^3 = 5S/12$ ,  $\sum_i [b/R_i^{(d)}]^3 = 7S/12$ ,  $\delta E_z^{(2)}$  turns out to be positive, as it should. The harmonic term in the  $(x, y)$  plane can again be computed but proves immaterial for the sake of our purposes. When all particles are shifted from their lattice positions  $\{\mathbf{R}_i\}$  to  $\{(x_i, y_i, z_i)\}$ , the total energy change is given, as far as the  $z$ -dependent contribution is concerned, by

$$- \beta \delta E \sim \frac{3^{3/4}}{(4\pi)^{3/2}} \frac{\sqrt{2}}{\sqrt{\Xi}} \frac{1}{2} \sum_{i < j} \frac{(\tilde{z}_i - \tilde{z}_j)^2}{(|\mathbf{R}_i - \mathbf{R}_j|/b)^3}. \quad (11)$$

Expanding  $\exp(-\beta \delta E)$  in  $1/\sqrt{\Xi}$  and enforcing electro-neutrality, the density profile  $\tilde{\rho}(\tilde{z})$  is obtained in the form

$$\tilde{\rho}(\tilde{z}) = \frac{2}{\tilde{d}} + \frac{1}{\theta} \frac{2}{\tilde{d}} \left[ \left( \tilde{z} - \frac{\tilde{d}}{2} \right)^2 - \frac{\tilde{d}^2}{12} \right] + O(\Xi^{-1}), \quad (12)$$

where

$$\theta = \frac{(4\pi)^{3/2}}{3^{3/4}} \frac{1}{S} \frac{\sqrt{\Xi}}{\sqrt{2}} = 1.252 \dots \sqrt{\Xi}. \quad (13)$$

This  $\theta$  differs from the single-plate one (9) by the factor  $1/\sqrt{2}$  due to the different hexagonal lattice spacings  $a$  and  $b$ . The functional form of (12) coincides with that of Moreira and Netz [10,11]. For (not yet asymptotic)  $\Xi = 100$ , the previous virial SC result  $\theta = \Xi$  is far away from the MC estimate  $\theta \approx 11.2$  [10], while our formula (13) gives  $\theta \approx 12.5$ .

Applying the contact-value theorem to the density profile (12), the pressure  $P$  between the plates is given by

$$\tilde{P} = \frac{\beta P}{2\pi\ell_B\sigma^2} = -1 + \frac{2}{\tilde{d}} + \frac{\tilde{d}}{3\theta} + O\left(\frac{\tilde{d}^2}{\Xi}\right). \quad (14)$$

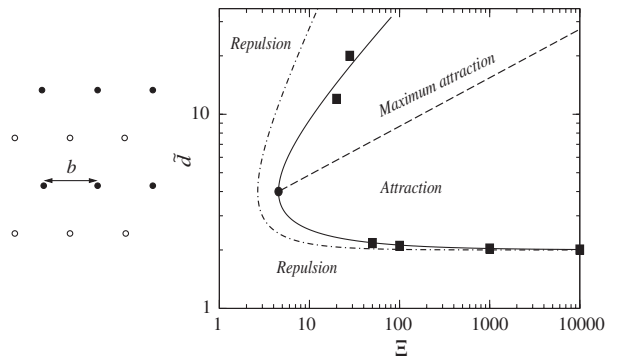


FIG. 2. Left: Structure I of counterions on two parallel charged plates (see text). Right: Phase diagram following from the equation of state (14): the solid curve shows the points where  $P = 0$ . The dash-dotted line is for the corresponding virial SC prediction [11]. The filled squares are those MC results from Ref. [10] with  $\Xi > 20$ , while the straight dashed line is for the points  $\tilde{d}_{\max}$  where  $\partial \tilde{P} / \partial \tilde{d} = 0$ .

An analogous result was obtained within the approximate approach of Ref. [17], with the underestimated ratio  $\theta/\sqrt{\Xi} = 3\sqrt{3}/2 \simeq 0.866$ . Equation (14) provides insight into the like-charge attraction phenomenon. The attractive ( $P < 0$ ) and repulsive ( $P > 0$ ) regimes are shown in Fig. 2 (right-hand panel). Although our results hold for  $\tilde{d} \ll \Xi^{1/2}$  and for large  $\Xi$ , the shape of the phase boundaries where  $P = 0$  (solid curve) shows striking similarity with its counterpart obtained numerically; the agreement with Monte Carlo data is good, and better than with the original virial SC prediction. While the upper branch of the attraction or repulsion boundary is such that  $\tilde{d}/\sqrt{\Xi}$  is of order unity and hence lies at the limit of validity of our expansion, we predict the maximum attraction to be obtained for  $\tilde{d}_{\max} = \sqrt{6\theta} \propto \Xi^{1/4}$ , as follows from enforcing  $\partial\tilde{P}/\partial\tilde{d} = 0$ . Since  $\tilde{d}_{\max}/\sqrt{\Xi} \propto \Xi^{-1/4} \rightarrow 0$ , we can consider the latter prediction, shown by the dashed line in Fig. 2, as asymptotically exact; we note that it is fully corroborated by the scaling laws reported in [15].

In conclusion, the present asymptotic result in the large  $\Xi$  regime shows that, while the leading order results (for one or two plates) can be obtained by a single counterion theory, the next terms actually reflect the complete ground-state structure ( $N$  counterion property). This explains the success of a virial-like expansion as in [11] to capture leading order effects, but its failure for higher order corrections. We have shown how such shortcomings can be circumvented within a physically transparent procedure and obtained analytical results in remarkable agreement with Monte Carlo data. Our exact results involve inverse powers of the expansion parameter  $\Xi$ ; in the two plates problem, our results apply under the double requirement that  $\Xi$  is large and that  $\tilde{d} < \sqrt{\Xi}$ .

Our approach bears similarities with that of Ref. [19], where, however, counterions have been assumed to stick to the plates. This assumption is certainly relevant at large  $\tilde{d}$ , but discards from the outset the excitations that are relevant in the complementary range  $\tilde{d} < \sqrt{\Xi}$ , where the counterions unbind from the plates; see above.

An important remark in order here is that the dominant results follow from a “single counterion” picture because, for a single *planar* interface, the dominant electric field stems from the plate only, while the counterion contribution is subdominant. The situation changes for a *curved* (say, spherical) interface since then other counterions contribute to the dominant field felt by a given ion, no matter how close to the interface this ion can be. Consequently, the dominant ion profile around a charged sphere will not be that obtained within the original approach of [10,11].

In practice, for a highly charged interface in water at room  $T$ , one has  $\sigma\ell_B^2 \simeq 1$ , so that  $\Xi$  may exceed 100 for trivalent or tetravalent counterions [12]. We also note that some highly charged systems, such as hydrated calciosilicates, responsible for the hardening of hydrated cement pastes, exhibit  $\Xi > 75$  already with divalent ions such as the commonly found  $\text{Ca}^{2+}$  [18]. Although asymptotic

(i.e., valid at large  $\Xi$ ), our predictions turn out to be reliable for such couplings. A generalization of the approach to dielectric inhomogeneities, systems with salt or asymmetric [24], offers interesting problems for more detailed studies in the future.

The support received from Grant VEGA No. 2/0113/2009 and CE-SAS QUTE is acknowledged.

---

\*On leave from: Institute of Physics, Slovak Academy of Sciences, Bratislava, Slovakia.

- [1] L. Guldbbrand, B. Jönson, H. Wennerström, and P. Linse, *J. Chem. Phys.* **80**, 2221 (1984); R. Kjellander and S. Marčelja, *Chem. Phys. Lett.* **112**, 49 (1984); P. Kékicheff, S. Marčelja, T. J. Senden, and V. E. Shubin, *J. Chem. Phys.* **99**, 6098 (1993).
- [2] V. A. Bloomfield, *Curr. Opin. Struct. Biol.* **6**, 334 (1996).
- [3] P. Linse and V. Lobaskin, *Phys. Rev. Lett.* **83**, 4208 (1999).
- [4] D. Andelman, in *Soft Condensed Matter Physics in Molecular and Cell Biology*, edited by W. C. K. Poon and D. Andelman (Taylor & Francis, New York, 2006).
- [5] P. Attard, D. J. Mitchell, and B. W. Ninham, *J. Chem. Phys.* **88**, 4987 (1988); **89**, 4358 (1988).
- [6] R. Podgornik, *J. Phys. A* **23**, 275 (1990).
- [7] R. R. Netz and H. Orland, *Eur. Phys. J. E* **1**, 203 (2000).
- [8] I. Rouzina and V. A. Bloomfield, *J. Phys. Chem.* **100**, 9977 (1996).
- [9] A. Y. Grosberg, T. T. Nguyen, and B. I. Shklovskii, *Rev. Mod. Phys.* **74**, 329 (2002); Y. Levin, *Rep. Prog. Phys.* **65**, 1577 (2002).
- [10] A. G. Moreira and R. R. Netz, *Phys. Rev. Lett.* **87**, 078301 (2001); *Eur. Phys. J. E* **8**, 33 (2002).
- [11] R. R. Netz, *Eur. Phys. J. E* **5**, 557 (2001).
- [12] A. Naji, S. Jungblut, A. G. Moreira, and R. R. Netz, *Physica (Amsterdam)* **352A**, 131 (2005).
- [13] R. Messina, *J. Phys. Condens. Matter* **21**, 113102 (2009).
- [14] S. Nordholm, *Chem. Phys. Lett.* **105**, 302 (1984).
- [15] Y. G. Chen and J. D. Weeks, *Proc. Natl. Acad. Sci. U.S.A.* **103**, 7560 (2006); J. M. Rodgers, C. Kaur, Y. G. Chen, and J. D. Weeks, *Phys. Rev. Lett.* **97**, 097801 (2006).
- [16] C. D. Santangelo, *Phys. Rev. E* **73**, 041512 (2006).
- [17] M. Hatlo and L. Lue, *Europhys. Lett.* **89**, 25002 (2010).
- [18] R. J.-M. Pellencq, J. M. Caillol, and A. Delville, *J. Phys. Chem. B* **101**, 8584 (1997).
- [19] A. W. C. Lau, D. Levine, and P. Pincus, *Phys. Rev. Lett.* **84**, 4116 (2000); A. W. C. Lau, P. Pincus, D. Levine, and H. A. Fertig, *Phys. Rev. E* **63**, 051604 (2001).
- [20] I. J. Zucker, *J. Math. Phys. (N.Y.)* **15**, 187 (1974); I. J. Zucker and M. M. Robertson, *J. Phys. A* **8**, 874 (1975).
- [21] G. Goldoni and F. M. Peeters, *Phys. Rev. B* **53**, 4591 (1996).
- [22] R. Messina and H. Löwen, *Phys. Rev. Lett.* **91**, 146101 (2003); E. C. Oğuz, R. Messina, and H. Löwen, *Europhys. Lett.* **86**, 28002 (2009).
- [23] V. Lobaskin and R. R. Netz, *Europhys. Lett.* **77**, 38003 (2007).
- [24] Y. S. Jho *et al.*, *Phys. Rev. Lett.* **101**, 188101 (2008); M. Kanduc *et al.*, *J. Chem. Phys.* **132**, 124701 (2010); *Phys. Rev. E* **78**, 061105 (2008).